Study of a Miniaturized Quasi-Self-Complementary UWB Antenna in Frequency and Time Domain

Lu GUO, Xiaodong CHEN, Clive PARINI

School of Electronic Engineering and Computer Science, Queen Mary, University of London, London, E1 4NS, UK.

lu.guo@elec.qmul.ac.uk, xiaodong.chen@elec.qmul.ac.uk, c.g.parini@elec.qmul.ac.uk

Abstract. *A compact antenna for UWB communication systems has been realized by employing a quasi-self-complementary structure together with a triangular notch on microstrip feed line in this paper. The optimal design of this type of antenna can offer an ultra wide return loss bandwidth with reasonable radiation properties. It features a quite small physical dimension of 16 mm×25 mm, corresponding to an electrically size of 0.24 λ. A good agreement is achieved between the simulated and the measured antenna characteristics. The major parameters that influence the performance of the antenna are investigated numerically to gain an insight into the antenna operation. Time domain performance of the antenna is also examined in order to assess its suitability for impulse radio applications.*

Keywords

Antenna transient analysis, self-complementary antennas, small antennas, UWB antennas.

1. Introduction

Small and compact UWB antennas are in high demand for various applications such as Wireless USB, indoor localization and on-body communications [1-3]. Various miniaturization techniques have been thus tried to design compact UWB antennas. For example, Zhining Chen et al. have designed a small swan-shaped UWB antenna by embedding a rectangular slot vertically from the printed radiator and asymmetrically attaching a strip to the radiator [4]. The antenna has achieved a -10 dB return loss bandwidth over 2.9 GHz – 11.6 GHz with a compact size of 25 mm×25 mm. Further miniaturization can be realized by adopting the substrate with a high dielectric constant. An example of such antenna has been developed by A. Abbosh et al [5]. The radiating element utilizes the intersection of an elliptical structure and is etched on a high dielectric constant substrate with ε_r=10.2 and thickness of 0.64 mm. The antenna exhibits a physical size of 20 mm×26 mm and features a -10 dB impedance bandwidth from 3.1 GHz to 15 GHz.

Apart from abovementioned techniques, another solution to miniaturize UWB antennas can be achieved by exploiting the self-complementary concept. Self-complementary antennas [6, 7] have illustrated their promising prospects with broadband characteristics. However, it is noted that a matching network is imperative to transform the input impedance from 188.5 to 50Ω in order to integrate with the RF front end. This has constrained the bandwidth of this type of antenna. For example, K. Wong et al. [8] have investigated a broadband printed quasi-self-complementary antenna, which is excited by a mini 50 Ω coaxial line, thus avoiding the extra matching circuit. However, the bandwidth of this antenna is only suitable for 5.2/5.8 GHz WLAN operation but not for UWB applications. Recently, our group has developed a printed quasi-self-complementary antenna that is fed by a 50Ω coaxial cable without using an extra matching circuit [9, 10]. The antenna demonstrates an ultra wide 10-dB impedance bandwidth as well as reasonable radiation patterns. It is also noticed that the antenna can be further reduced for easy integration into space-limited systems.

This paper presents our study on a compact printed quasi-self-complementary antenna fed by a microstrip line without employing a matching circuit. A triangular slot is notched on the ground plane to improve the impedance matching of the antenna. Critical parameters that affect the performance of the antenna are investigated to gain an insight into antenna operation. Importantly, the proposed antenna features not only physically small size of 16 mm×25 mm but also electrically small size of 0.24 λ. It has been shown that the antenna generally exhibits a good performance in both frequency and time domain.

2. Background of Self-Complementary Antenna

The self-complementary antenna (SCA), firstly proposed by Mushiake [11, 12], has claimed a broad impedance bandwidth. Theoretically, a self-complementary antenna possesses the constant input impedance 188.5 Ω, independent of the source frequency and the antenna configuration. As described in [13], a pair of complementary slot and dipole antennas is shown in Fig. 1.

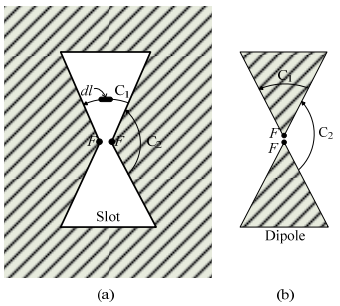

Fig. 1. Slot antenna (a) and complementary dipole antenna (b)

The terminals of each antenna are denoted by *FF*, as shown in Fig. 1 (a) and (b) respectively, and it is assumed that they are separated by an infinitesimal distance. It is also assumed that the slot and dipole are cut from an infinitesimally thin, plane, perfectly conducting sheet. The driving-point impedance Z_S at the terminals of the slot antenna in Fig. 1 (a) is the ratio of the terminal voltage V_S to the terminal current I_S while Z_d is the ratio of the terminal voltage V_d to the terminal current I_d of the dipole antenna in Fig. 1 (b). After derivations in [13], it is found that

$$Z_s Z_d = \frac{Z_0^{\,2}}{4} \tag{1}$$

where Z_0 is the intrinsic impedance of the surrounding medium. Equation (1) indicates that the terminal impedance Z_S of a slot antenna is equal to quarter of the square of the intrinsic impedance of the surrounding medium divided by the terminal impedance Z_d of the complementary dipole antenna [13].

It is seen in (1) that the product of the impedances of two complementary antennas is the constant $Z_0^2/4$. If the antenna is its own complement, frequency-independent impedance behavior can be achieved. This is the self-complementary property, in which the antenna and its complement are identical. A self-complementary structure can be made to exactly overlay its complement through translation and/or rotation. The value of impedance follows directly from (1), as noted by Mushiake:

$$Z = Z_s = Z_d = \frac{Z_0}{2} = 188.5\Omega\,. \tag{2}$$

Therefore, in theory, a perfect self-complementary antenna on an infinitely large plane has the constant input impedance 188.5 Ω, independent of the source frequency and the antenna shape. However, in practice, a self-complementary antenna has to be truncated on a finite plane, which limits its bandwidth. Furthermore, an impedance matching circuit for transforming 188.5 Ω to 50 Ω will further narrow the bandwidth and limit the reduction of antenna size. Hence, we have proposed a novel approach to design a quasi-self-complementary structure for a direct 50Ω feeding. The design procedure is similar to the one illustrated in [10], where an evolution of the CPW-Fed quasi-self-complementary antenna is elaborated. However, in this paper, a slotted microstrip line rather than a CPW feeding is proposed.

The design procedure of the proposed antenna is depicted in Fig. 2. As the starting point, a half circular disc and its slot counterpart are printed on the different side of the substrate, which resembles a truncated self-complementary structure, as shown in Fig. 2 (a). A 50 Ω microstrip line is then added to feed the original geometry, as displayed in Fig. 2 (b). Lastly, a triangular notch is inserted on the microstrip line for the purpose of improving impedance matching, as illustrated in Fig. 2 (c).

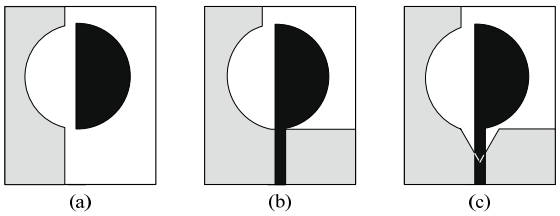

Fig. 2. Design procedure of the microstrip fed quasi-self-complementary antenna.

3. Antenna Design and Performance

3.1 Antenna Geometry and Performance

The compact quasi-self-complementary UWB antenna investigated in this paper is displayed in Fig. 3. A half circular disc with a radius of *r* and its complementary magnetic counterpart are printed on the different side of the dielectric substrate (in this study, the FR4 substrate of thickness $H = 1.6$ mm and relative permittivity $\varepsilon_r = 3.0$ was used). *L* and *W* denote the length and the width of the dielectric substrate, respectively. Additionally, in order to enhance the impedance matching of the antenna, a triangular notch is proposed on the ground plane. W_S and L_2 represent the width and height of the triangular notch respectively. The simulations are performed using the CST Microwave Studio® package which adopts the Finite Integration Technique for electromagnetic computation [14]. The prototype of microstrip line-fed quasi-self-complementary antenna with optimal design, i.e. $r = 6$ mm, $W = 16$ mm, $L = 25$ mm, $W_S = 6$ mm, $W_f = 2.4$ mm, $L_1 = 8.9$ mm, $L_2 = 4.8$ mm, as shown in Fig. 3, is built in the Antenna Measurement Laboratory at Queen Mary, University of London (QMUL). The return losses are measured by using a HP 8720ES network analyzer and the radiation pattern measurements are carried out inside an anechoic chamber.

Fig. 4 depicts the simulated and the measured return loss curves. The simulated bandwidth spans from 2.8 GHz to 11.3 GHz. This UWB characteristic of the quasi-self-complementary antenna is verified in the measurement, with bandwidth spanning from 2.86 GHz to 10.7 GHz. It is noticed that the discrepancy between the simulation and the measurement is due to the effect of the feeding cable since the antenna is rather small. The feeding cable effect has been verified both numerically and experimentally. It is also noticed that the antenna size is not only physically

small but also electrically small, only 0.24λ at 2.86 GHz, as shown in Fig. 3 (b). Tab. 1 illustrates the comparison of the features between the proposed antenna and other UWB antennas proposed elsewhere.

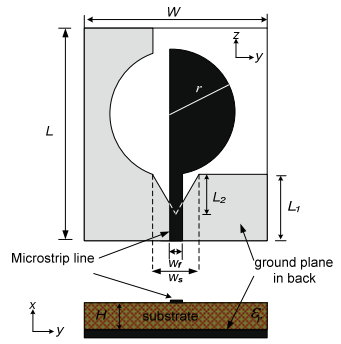

(a)

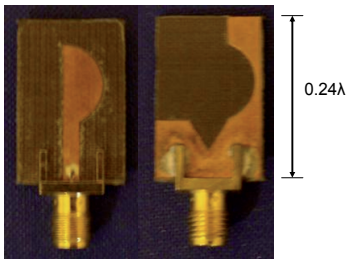

(b)

Fig. 3. The proposed microstripline-fed quasi-self-complementary antenna: (a) Geometry and (b) Prototype.

	Bandwidth (GHz)	Physical size (mm)	Electrical size
Proposed antenna	2.86 – 10.7	25×16	0.24λ
Antenna in [4]	2.95 – 11.6	25×25	0.25λ
Antenna in [5]	3.1 – 15	26×20	0.27λ

Tab. 1. Comparison of features between the proposed antenna and other UWB antennas.

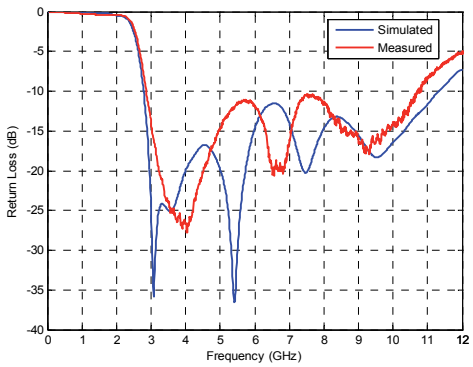

Fig. 4. Simulated (blue) and measured (red) return loss curves.

The measured and the simulated normalized radiation patterns at 3.07 GHz and 9.31 GHz are shown in Fig. 5 and Fig. 6, respectively. The patterns obtained in the measurement are close to those in the simulation. The minor discrepancy is again due to the feeding cable effect, particularly at low frequencies. It is observed that the *H*-plane patterns are reasonable over the entire operating bandwidth. The simulated peak gain of the proposed antenna is plotted in Fig. 7. It is illustrated that a satisfactory gain level is achieved through the whole band.

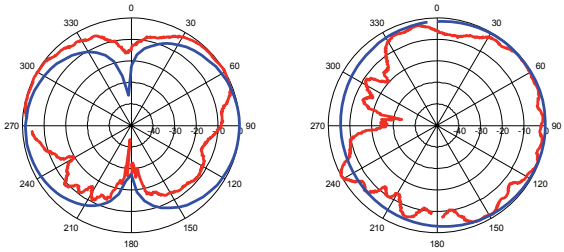

Fig. 5. Simulated (blue) and measured (red) radiation patterns with the optimal design at 3.07 GHz: (a) *E*-plane, (b) *H*-plane.

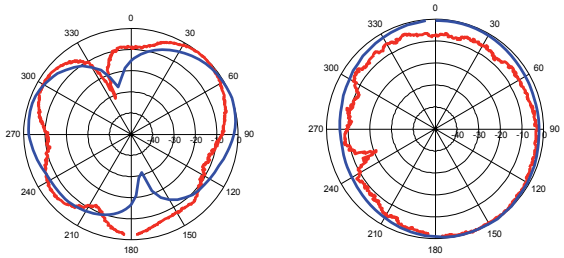

Fig. 6. Simulated (blue) and measured (red) radiation patterns with the optimal design at 9.31 GHz: (a) *E*-plane, (b) *H*-plane.

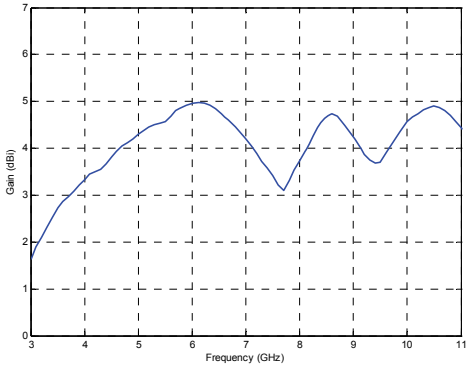

Fig. 7. Simulated peak gain of the proposed antenna.

3.2 Effects of Design Parameters

It has been noticed in the simulation that the operating bandwidth of the printed quasi-self-complementary antenna is critically dependent on the width of the antenna W, the width of the triangular notch W_S and the height of the notch L_2. So these parameters should be optimized for maximum bandwidth.

(i) The Effect of Antenna Width *W*

Fig. 8 depicts the simulated return loss curves with different antenna width (W=15, 16, 20 and 24 mm) when W_S is fixed at 6 mm and L_2 at 4.8 mm, respectively. It is noticed that the return loss curves vary significantly for the four different W. When W is narrowed, the first resonant frequency does not change much, however the higher resonant frequencies vary dramatically, leading to the variations of the operating bandwidth of the antenna. It is also interestingly observed that when the width W increases, the impedance matching at the lower band degrades. This is owing to the fact that the antenna will more and more resemble a genuine self-complementary structure with the extension of the width W. This results in the antenna impedance more approaching to 188.5 Ω and consequently the mismatch of the input impedance to the microstrip line. Basically, the notched microstrip line acts as a built-in transformer between the self-complementary structure and the SMA. The optimal antenna width is found to be at W = 16 mm.

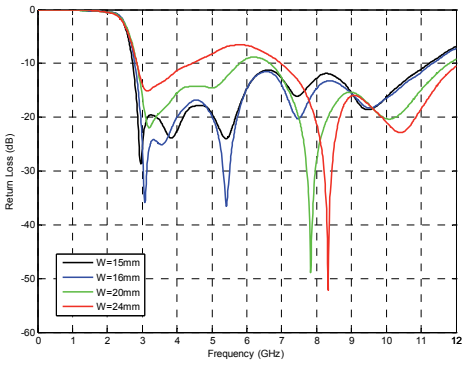

Fig. 8. Simulated return loss curves for different widths of the ground plane with W_S = 6 mm and L_2 = 4.8 mm.

(ii) The Effect of the Width of the Triangular Notch W_S

The simulated return loss curves with L_2 = 4.8 mm and optimal antenna width W of 16 mm for different triangular notch widths W_S are illustrated in Fig. 9. When W_S = 2 mm, it's close to a regular microstrip line so the impedance matching is not good over the entire band, as shown in blue curve in Fig. 9. When W_S increases from 2 mm to 6 mm the impedance matching of the antenna gets better, however the higher edge of the bandwidth decreases. With the further increase of W_S from 6 mm to 8 mm the impedance matching of the antenna worsens and the higher end of the bandwidth keeps reducing. It has been noticed that the size of the slot formed by the bottom edge of the half disc and the triangular notch is vital to the impedance matching of the antenna. With an appropriate size of the slot the traveling wave can be supported well, therefore leading to a good impedance matching of the antenna, as has been addressed in our previous paper [11]. This fact gives further indication that an even better impedance matching can be obtained by properly smoothing the edges of the triangular notch. It is also seen in Fig. 9 that the first resonance remains at around 3 GHz for different W_S, thus the change of W_S would not influence the lower band performance of the antenna. The optimized triangular slot width is found to be at W_S = 6 mm.

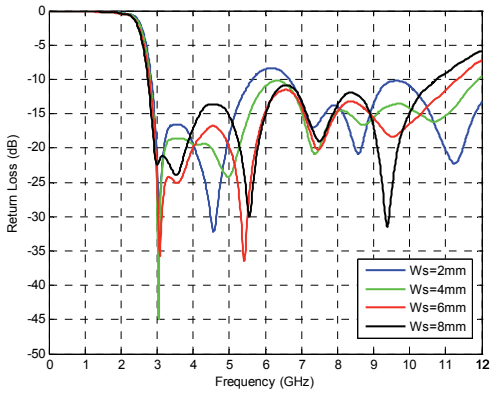

Fig. 9. Simulated return loss curves for different widths of the triangular slot with W = 16 mm and L_2 = 4.8 mm.

(iii) The Effect of the Height of the Triangular Notch L_2

Fig. 10 displays the simulated return loss curves for different notch height L_2 when W = 16 mm and W_S = 6 mm, respectively. When L_2 is equal to 4.8 mm, the -10 dB bandwidth covers an ultra wide frequency band, as shown in red curve in Fig. 10; when L_2 decreases to 2.8 mm and 0.8 mm, the lower edge of the bandwidth increases and the impedance matching for L_2 = 0.8 mm becomes worse as it's more approaching to a regular microstrip line. When L_2 rises to 6.8 mm the lower edge of the bandwidth reduces, however, the impedance matching for mid band is degraded. Therefore, L_2 would affect both the impedance matching and the lower band performance of the antenna.

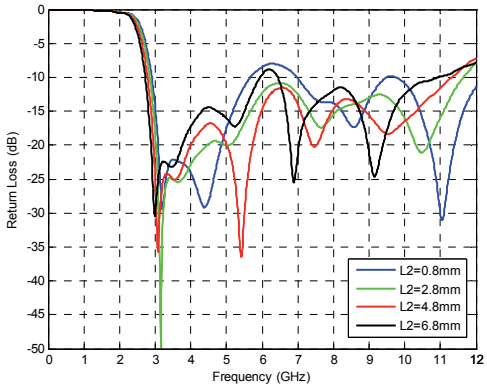

Fig. 10. Simulated return loss curves for different heights of the triangular slot with W = 16 mm and W_S= 6 mm.

4. Time Domain Behaviors of the Antenna

4.1 System Set-up

The antenna system consists of two identical quasi-self-complementary UWB antennas, as shown in Fig. 11.

The antenna pair is vertically placed, and the distance between them is set to 1000 mm. Two different orientations will be investigated, namely face-to-face and side-by-side, as depicted in Fig. 11. The "face" side is the front side featuring the half circular disc and side-by-side orientation features an alignment as shown in Fig. 3 (b).

Fig. 11. Two antenna pair orientations.

4.2 Source Pulse

In this study, two kinds of pulse are selected as the input signal. One is the first-order Rayleigh pulse which has the form of equation (3)

$$f(t) = -\frac{2t}{a^2} e^{-\left(\frac{t}{a}\right)^2} \tag{3}$$

where, the pulse parameter a denotes the characteristic time. Large a corresponds to wide waveform in the time domain but narrow bandwidth in the frequency domain. $a = 45$ ps is selected in this study, its time domain waveform and frequency domain power spectral density (PSD) are shown in Fig. 12 and Fig. 13, respectively. It is clearly seen that the spectrum of this pulse doesn't fully fall into the UWB band defined by the FCC, i.e. 3.1-10.6 GHz.

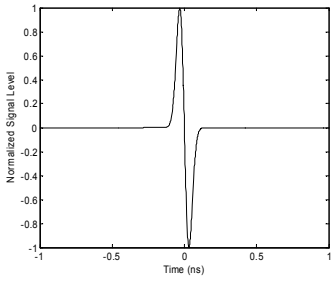

Fig. 12. The waveform of first-order Rayleigh pulse (a= 45 ps).

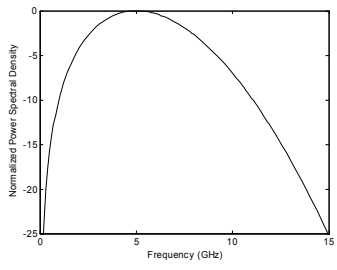

Fig. 13. The PSD of first-order Rayleigh pulse (a = 45 ps).

Another input signal has the form of equation (4).

$$f(t) = \sin(2\pi f_c t) e^{-(t/a)^2} . \tag{4}$$

f_c is the carrier frequency and a still represents the characteristic time. f_c = 4 GHz and a = 300 ps are selected in order to make its spectrum fully locate within the bandwidth of the antenna system. The waveform and PSD of the modulated input pulse are depicted in Fig. 14 and Fig. 15, respectively.

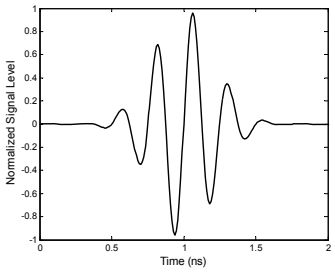

Fig. 14. The waveform of modulated signal.

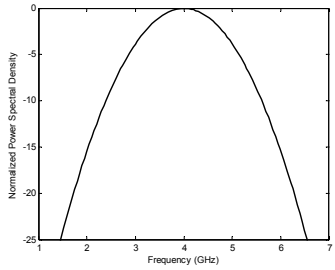

Fig. 15. The PSD of modulated signal.

4.3 Measured Received Pulse

The antenna system can be modeled as a linear, time invariant system, therefore the received signal can be obtained by convolving the input pulse and the impulse response of the antenna system. In this study, the transfer function (magnitude together with group delay) for side-by-side orientation is measured using a HP 8720ES network analyzer, as shown in Fig. 16. It is clearly noticed that within 2.5~7 GHz frequency band, the magnitude of the transfer function is relatively flat and the group delay is nearly a constant. The transfer function is firstly transformed to the time domain by performing the Inverse Fourier Transform, it is then convolved with the input pulse, and the measured UWB signal is consequently obtained. Fig. 17 illustrates the comparison of the received pulse and the input pulse for two different excited pulses, respectively. For comparison purpose, the input pulse has been shifted up along the time axis to coincide with the received signal. It is clearly shown that for the modulated input signal, it is almost distortionless, however, for the first-order Rayleigh input signal, it is spread and severely distorted. This can be explained by the antenna's filtering characteristic. The main energy of modulated input signal is completely within the operating band of the antenna system, thus the antenna system just serves as a band-pass filter. However, in the first-order Rayleigh input signal scenario, since its energy is partly distributed outside the working band of the antenna system, it will definitely suffer the distortion. Thus, it is important to know the input signal while designing the antenna system.

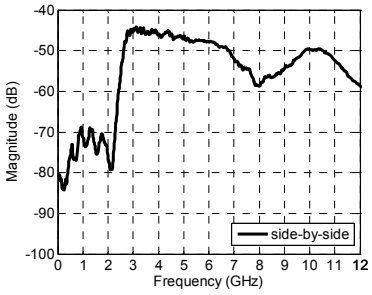

(a)

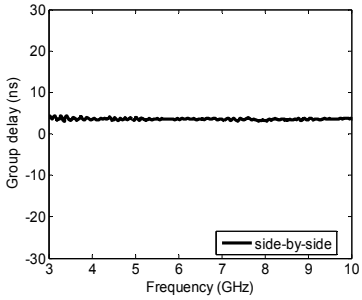

(b)

Fig. 16. (a) Measured magnitude of transfer function S_{21} and (b) group delay of transfer function S_{21}.

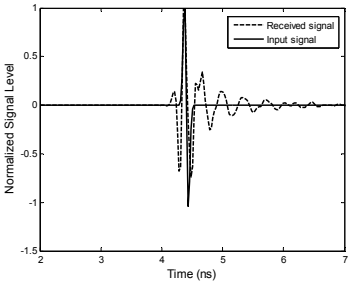

(a)

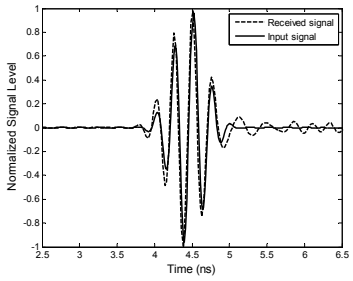

(b)

Fig. 17. Comparison of the received pulse and the input pulse for two different excited signals (a) First-order Rayleigh pulse input, (b) Modulated signal input.

Apart from the side-to-side orientation, the face-to-face orientation is also investigated. Only the modulated input signal is considered here. Fig. 18 plots the measured received signal for these orientations and it is seen that the received pulses are almost identical.

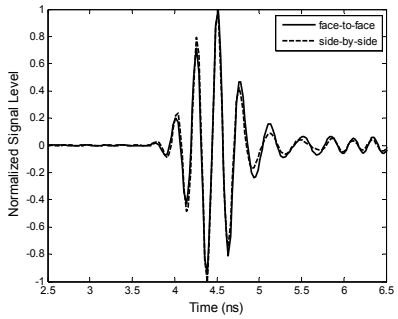

Fig. 18. Received signal for different antenna orientations.

5. Conclusion

A compact printed quasi-self-complementary UWB antenna is investigated in this paper. It is demonstrated numerically and experimentally that the proposed printed microstripline-fed quasi-self-complementary antenna can achieve an ultrawide impedance bandwidth, from 2.86 GHz to 10.7 GHz. It also exhibits small dimensions: 16 mm×25 mm in physical size and 0.24λ in electrical size, respectively. The key parameters that influence antenna performance have been analyzed to gain an insight into antenna operation. A time domain study of the antenna is also conducted. It is shown that the small quasi-self-complementary antenna generally exhibits a good performance in both frequency and time domain and therefore is a good candidate for UWB applications.

Acknowledgements

The authors would like to thank John Dupuy, Hansheng Su and Xiaoming Liu of the Department of Electronic Engineering, QMUL for their help on the measurement of the antenna. The authors would like to acknowledge Computer Simulation Technology (CST), Germany, for the complimentary license of the trademarked Microwave Studio package.

References

[1] VIANI, F., LIZZI, L., AZARO, R., MASSA, A. A Miniaturized UWB antenna for wireless dongle devices. *IEEE Antennas and Wireless Propagation Letters,* 2008, vol. 7, p. 714 - 717.

[2] CHEN, Z., SEE, T. Small UWB antennas for wireless USB dongle attached to laptop computer. In *IEEE International Workshop on Antenna Technologies: Small and Smart Antennas Metamaterials and Applications (IWAT 2007).* Cambridge (UK), 21-23, March 2007.

[3] KLEMM, M., TROESTER, G. Textile UWB antennas for wireless body area networks. *IEEE Transaction on Antennas and Propagation,* 2006, vol. 54, no. 11, p. 3192-3197.

[4] CHEN, Z., SEE, T., QING, X. Small printed ultrawideband antenna with reduced ground plane effect. *IEEE Transaction on Antennas and Propagation*, 2007, vol. 55, no. 2, p. 383-388.

[5] ABBOSH, A., BIALKOWSKI, M., JACOB, M., MAZIERSKA, J. Design of a compact ultra wideband antenna. *Microw. Opt. Technol. Lett*., 2006, vol. 48, p. 1515-1518.

[6] XU, P., FUJIMOTO, K., LIN, S. Performance of quasi-selfcomplementary antenna using a monopole and a slot. In *2002 IEEE Antennas and Propagation Society Int. Symp*. San Antonio (TX, USA), June 2002.

[7] KUROKI, F., OHTA, H., YAMAGUCHI, M., SUEMATSU, E. Wall-hanging type of self-complementary spiral patch antenna for indoor reception of digital terrestrial broadcasting. *IEEE MTT-S Int. Microw. Symp. Dig*., 2006, p. 194-197.

[8] WONG, K., WU, T., SU, S., LAI, J. Broadband printed quasi-self-complementary antenna for 5.2/5.8 GHz WLAN operation. *Microw. Opt. Technol. Lett*., 2003, vol. 39, no. 6, p. 495-496.

[9] GUO, L., WANG, S., GAO, Y., WANG, Z., CHEN, X., PARINI, C. Study of a printed quasi-self-complementary antenna for ultra wideband systems. *IET Electronic Letters*, 2008, vol. 44, no. 8, p. 511-512.

[10] GUO, L., CHEN, X., PARINI, C. A printed quasi-self-complementary antenna for UWB applications. In *2008 IEEE AP-S International Symposium on Antenna and Propagation*. San Diego (USA), 5-12, July 2008.

[11] MUSHIAKE, Y. Self-complementary antennas. *IEEE Antennas Propag. Mag*., 1992, vol. 34, no. 6, p. 23-29.

[12] MUSHIAKE, Y. A report on Japanese development of antennas: from the Yagi-Uda antenna to self-complementary antennas. *IEEE Antennas Propag. Mag*., 2004, vol. 46, no. 4, p. 47-60.

[13] KRAUS, J. *Antennas for All Applications*. McGraw-Hill, Inc., 2002.

[14] User's manual. CST-Microwave Studio, 2003.